Research in Astronomy and Astrophysics, 22:125001 (7pp), 2022 December https://doi.org/10.1088/1674-4527/ac8de5

The Analytical Equation of the Three-point Correlation Function of Galaxies: to the Third Order of Density Perturbation

Shu-Guang Wu and Yang Zhang
Department of Astronomy, Key Laboratory for Researches in Galaxies and Cosmology, University of Science and Technology of China, Hefei 230026, China
wusg@mail.ustc.edu.cn, yzh@ustc.edu.cn
Received 2022 June 16; revised 2022 August 1; accepted 2022 August 10; published 2022 November 11

Abstract

Applying functional differentiation to the density field with Newtonian gravity, we obtain the static, nonlinear equation of the three-point correlation function ζ of galaxies to the third order density perturbations. We make the equation closed and perform renormalization of the mass and the Jeans wavenumber. Using the boundary condition inferred from observations, we obtain the third order solution $\zeta(r, u, \theta)$ at fixed $u = 2$, which is positive, exhibits a U-shape along the angle θ, and decreases monotonously along the radial r up to the range $r \leqslant 30\, h^{-1}$ Mpc in our computation. The corresponding reduced $Q(r, u, \theta)$ deviates from 1 of the Gaussian case, has a deeper U-shape along θ, and varies non-monotonously along r. The third order solution agrees with the SDSS data of galaxies, quite close to the previous second order solution, especially at large scales. This indicates that the equations of correlation functions with increasing orders of density perturbation provide a stable description of the nonlinear galaxy system.

Key words: (cosmology:) large-scale structure of universe – hydrodynamics – gravitation

1. Introduction

In study of the distribution of galaxies, the n-point correlation functions (nPCF) are important tools which contain the dynamical and statistical information of the system of galaxies (Groth & Peebles 1975, 1977; Fry & Peebles 1978; Peebles 1980, 1993; Fry 1983, 1984, 1994; Bernardeau et al. 2002). The analytical, closed equations of the 2PCF ξ (also denoted as $G^{(2)}$) up to the second order of density perturbation have been derived for the static case (Zhang 2007; Zhang & Miao 2009; Zhang & Chen 2015; Zhang et al. 2019), as well as for the evolution case (Zhang & Li 2021). The associated solutions have simultaneously provided simple explanations of several seemingly-unrelated features of the observed correlation of galaxies, such as the power law of the correlation $\xi \simeq (r_0/r)^{1.7}$ in a range $r = (0.1 \sim 10)\, h^{-1}$ Mpc, the correlation amplitude being proportional to the galaxy mass $\xi \propto m$, the correlation function of clusters having a similar form to that of galaxies $\xi_{cc} \simeq (10 \sim 20)\xi_{gg}$ with a higher amplitude, the scaling behavior of the cluster correlation amplitude, the 100 Mpc-periodic bumps of the observed $\xi_{gg}(r)$ on very large scales, the small wiggles in the power spectrum caused by acoustic oscillating waves, etc. The statistic of galaxy distribution is non-Gaussian due to long-range gravity, and $G^{(2)}$ is insufficient to reveal the non-Gaussianity. It is necessary to study the 3PCF $G^{(3)}(\boldsymbol{r}, \boldsymbol{r}', \boldsymbol{r}'')$ which statistically describes the excess probability over random of finding three galaxies located at the three vertices $(\boldsymbol{r}, \boldsymbol{r}', \boldsymbol{r}'')$ of a given triangle (Fry & Peebles 1978; Peebles 1980; Fry 1984). There are a few preliminary analytical studies of $G^{(3)}$. Fry (1984) did not give the equation of $G^{(3)}$ and tried to calculate $G^{(3)}$ to the lowest non-vanishing order in density perturbation, assuming initial conditions that are Gaussian and have a power-law spectrum. Similarly, using the BBGKY hierarchy, Inagaki (1991) calculated the Fourier transformation of $G^{(3)}$ perturbatively under Gaussian initial conditions. For the system of galaxies, however, its non-Gaussian distribution function is unknown, so that generally one is not able to compute $G^{(3)}$ even if the density perturbation as one realization is given. Besides, the initial power spectrum of the system of galaxies is not of a simple power-law form even at the early epoch when galaxies are newly formed at some high redshifts. Bharadwaj (1994, 1996) adopted the BBGKY hierarchy method and formally wrote down an equation of $G^{(3)}$ for a Newtonian gravity fluid without pressure and vorticity. But the formal equation contains no pressure and source terms and will not be able to exhibit oscillation and clustering properties. Moreover, the formal equation is not closed yet and involves other unknown functions beside $G^{(3)}$. This situation is similar to that in Davis & Peebles (1977), which gave an equation for $G^{(2)}$ involving other unknown functions. These unclosed equations are hard to use for the actual system of galaxies, since appropriate initial conditions are difficult to specify for several unknown functions. In Wu & Zhang (2022) the static equation of $G^{(3)}$ was studied to the second order of density perturbation, and the solution describes the overall profile of the observed 3PCF (Marín 2011). In this paper, we will work on the third order density perturbation, and also give renormalization of the mass m and the Jeans wavenumber, and compare the solution with observations.

Within a small redshift range, the expansion effect is small, and the correlations of galaxies can be well described by the static equation. As demonstrated for the case of 2PCF

(Zhang & Li 2021), the expansion term in the evolution equation is about two orders smaller than the pressure and gravity terms, and the 2PCF increases slowly, $\xi \propto (1+z)^{-0.2}$ for $z = 0.5 \sim 0.0$.

2. Equation of 3PCF to Third Order of Density Perturbation

The equation of the density field with Newtonian gravity (Zhang 2007; Zhang & Miao 2009; Zhang & Chen 2015; Zhang et al. 2019; Wu & Zhang 2022)

$$\nabla^2\psi - \left(\frac{\nabla\psi}{\psi}\right)^2 + k_J^2\psi^2 + J\psi^2 = 0, \tag{1}$$

where $\psi(\boldsymbol{r}) \equiv \rho(\boldsymbol{r})/\rho_0$ is the rescaled mass density field with ρ_0 being the mean mass density, $k_J \equiv (4\pi G\rho_0/c_s^2)^{1/2}$ is the Jeans wavenumber, c_s is the sound speed, and J is the external source employed to carry out functional derivatives conveniently. The n-point correlation function is defined by $G^{(n)}(\boldsymbol{r}_1,\cdots,\boldsymbol{r}_n) = \langle\delta\psi(\boldsymbol{r}_1)\cdots\delta\psi(\boldsymbol{r}_n)\rangle = \frac{1}{\alpha^{n-1}}\frac{\delta^{n-1}\langle\psi(\boldsymbol{r}_1)\rangle}{\delta J(\boldsymbol{r}_2)\cdots\delta J(\boldsymbol{r}_n)}|_{J=0}$, where $\delta\psi(\boldsymbol{r}) = \psi(\boldsymbol{r}) - \langle\psi\rangle$ is the fluctuation around the expectation value $\langle\psi\rangle$, and $\alpha = c_s^2/4\pi Gm$. (See Binney et al. 1992; Goldenfeld 1992; Zinn-Justin 1996; Zhang 2007; Zhang & Miao 2009; Zhang & Chen 2015; Zhang et al. 2019; Zhang & Li 2021.) To derive the equation of $G^{(3)}(\boldsymbol{r}, \boldsymbol{r}', \boldsymbol{r}'')$, we take the ensemble average of Equation (1) in the presence of J, and take the functional derivative of this equation twice with respect to the source J, and set $J = 0$. The second term in Equation (1) is expanded as

$$\begin{aligned}\left\langle\frac{(\nabla\psi)^2}{\psi}\right\rangle &= \frac{(\nabla\langle\psi\rangle)^2}{\langle\psi\rangle} + \frac{\langle(\nabla\delta\psi)^2\rangle}{\langle\psi\rangle} - \frac{\nabla\langle\psi\rangle}{\langle\psi\rangle^2}\cdot\langle\nabla(\delta\psi)^2\rangle \\ &+ \frac{(\nabla\langle\psi\rangle)^2}{\langle\psi\rangle^3}\langle(\delta\psi)^2\rangle \\ &- \frac{1}{\langle\psi\rangle^2}\langle\delta\psi(\nabla\delta\psi)^2\rangle + \frac{2}{3}\frac{1}{\langle\psi\rangle^3}\nabla\langle\psi\rangle\cdot\langle\nabla(\delta\psi)^3\rangle \\ &- \frac{(\nabla\langle\psi\rangle)^2}{\langle\psi\rangle^4}\langle(\delta\psi)^3\rangle + \cdots\end{aligned} \tag{2}$$

containing $(\delta\psi)^3$, higher than our previous work (Wu & Zhang 2022). Calculations yield the following equation

$$\begin{aligned}&\left(1 + \frac{1}{\psi_0^2}G^{(2)}(0)\right)\nabla^2 G^{(3)}(\mathbf{r}, \mathbf{r}', \mathbf{r}'') \\ &+ \left(\frac{2}{\psi_0^2}\nabla G^{(2)}(0) - \frac{2}{\psi_0^3}\nabla G^{(3)}(0)\right)\cdot\nabla G^{(3)}(\mathbf{r}, \mathbf{r}', \mathbf{r}'') \\ &+ \left(2k_J^2\psi_0 + \frac{1}{2\psi_0^2}\nabla^2 G^{(2)}(0) - \frac{2}{3\psi_0^3}\nabla^2 G^{(3)}(0)\right. \\ &\left. - \frac{1}{\psi_0^2}k_J^2 G^{(3)}(0)\right)G^{(3)}(\mathbf{r}, \mathbf{r}', \mathbf{r}'') \\ &+ \frac{1}{2\psi_0^2}G^{(2)}(\mathbf{r}, \mathbf{r}'')\nabla^2 G^{(3)}(\mathbf{r}, \mathbf{r}, \mathbf{r}') \\ &+ \frac{1}{2\psi_0^2}G^{(2)}(\mathbf{r}, \mathbf{r}')\nabla^2 G^{(3)}(\mathbf{r}, \mathbf{r}, \mathbf{r}'') \\ &+ \frac{2}{\psi_0^2}\nabla G^{(3)}(\mathbf{r}, \mathbf{r}, \mathbf{r}')\cdot\nabla G^{(2)}(\mathbf{r}, \mathbf{r}'') \\ &+ \frac{2}{\psi_0^2}\nabla G^{(2)}(\mathbf{r}, \mathbf{r}')\cdot\nabla G^{(3)}(\mathbf{r}, \mathbf{r}, \mathbf{r}'') \\ &+ \frac{1}{\psi_0^2}G^{(3)}(\mathbf{r}, \mathbf{r}, \mathbf{r}')\nabla^2 G^{(2)}(\mathbf{r}, \mathbf{r}'') \\ &+ \frac{1}{\psi_0^2}G^{(3)}(\mathbf{r}, \mathbf{r}, \mathbf{r}'')\nabla^2 G^{(2)}(\mathbf{r}, \mathbf{r}') \\ &- \frac{1}{2\psi_0}\nabla^2 G^{(4)}(\mathbf{r}, \mathbf{r}, \mathbf{r}', \mathbf{r}'') \\ &- \frac{2}{3\psi_0^3}G^{(2)}(\mathbf{r}, \mathbf{r}'')\nabla^2 G^{(4)}(\mathbf{r}, \mathbf{r}, \mathbf{r}, \mathbf{r}') \\ &- \frac{2}{3\psi_0^3}G^{(2)}(\mathbf{r}, \mathbf{r}')\nabla^2 G^{(4)}(\mathbf{r}, \mathbf{r}, \mathbf{r}, \mathbf{r}'') \\ &- \frac{2}{\psi_0^3}\nabla G^{(2)}(\mathbf{r}, \mathbf{r}'')\cdot\nabla G^{(4)}(\mathbf{r}, \mathbf{r}, \mathbf{r}, \mathbf{r}') \\ &- \frac{2}{\psi_0^3}\nabla G^{(2)}(\mathbf{r}, \mathbf{r}')\cdot\nabla G^{(4)}(\mathbf{r}, \mathbf{r}, \mathbf{r}, \mathbf{r}'') \\ &- \frac{1}{\psi_0^2}k_J^2 G^{(2)}(\mathbf{r}, \mathbf{r}'')G^{(4)}(\mathbf{r}, \mathbf{r}, \mathbf{r}, \mathbf{r}') \\ &- \frac{1}{\psi_0^2}k_J^2 G^{(2)}(\mathbf{r}, \mathbf{r}')G^{(4)}(\mathbf{r}, \mathbf{r}, \mathbf{r}, \mathbf{r}'') \\ &- \frac{2}{\psi_0}\left(1 + \frac{3}{\psi_0^2}G^{(2)}(0) - \frac{3}{\psi_0^3}G^{(3)}(0)\right) \\ &\times\nabla G^{(2)}(\mathbf{r}, \mathbf{r}')\cdot\nabla G^{(2)}(\mathbf{r}, \mathbf{r}'') \\ &+ \left(2k_J^2 - \frac{1}{\psi_0^3}\nabla^2 G^{(2)}(0) + \frac{2}{\psi_0^4}\nabla^2 G^{(3)}(0)\right. \\ &\left. + \frac{2}{\psi_0^3}k_J^2 G^{(3)}(0)\right)G^{(2)}(\mathbf{r}, \mathbf{r}')G^{(2)}(\mathbf{r}, \mathbf{r}'') \\ &- \left(\frac{4}{\psi_0^3}\nabla G^{(2)}(0) - \frac{6}{\psi_0^4}\nabla G^{(3)}(0)\right)\cdot(\nabla G^{(2)}(\mathbf{r}, \mathbf{r}')G^{(2)}(\mathbf{r}, \mathbf{r}'') \\ &+ \nabla G^{(2)}(\mathbf{r}, \mathbf{r}'')G^{(2)}(\mathbf{r}, \mathbf{r}')) \\ &- \frac{2}{\psi_0^3}G^{(2)}(0)(G^{(2)}(\mathbf{r}, \mathbf{r}')\nabla^2 G^{(2)}(\mathbf{r}, \mathbf{r}'') \\ &+ G^{(2)}(\mathbf{r}, \mathbf{r}'')\nabla^2 G^{(2)}(\mathbf{r}, \mathbf{r}')) \\ &= -\frac{\psi_0}{\alpha}\left[\left(2 - \frac{1}{\psi_0^3}G^{(3)}(0)\right)G^{(2)}(\mathbf{r}, \mathbf{r}')\right. \\ &\left. + \frac{1}{\psi_0^2}G^{(4)}(\mathbf{r}, \mathbf{r}, \mathbf{r}, \mathbf{r}')\right]\delta^{(3)}(\mathbf{r} - \mathbf{r}'') \\ &- \frac{\psi_0}{\alpha}\left[\left(2 - \frac{1}{\psi_0^3}G^{(3)}(0)\right)G^{(2)}(\mathbf{r}, \mathbf{r}'')\right. \\ &\left. + \frac{1}{\psi_0^2}G^{(4)}(\mathbf{r}, \mathbf{r}, \mathbf{r}, \mathbf{r}'')\right]\delta^{(3)}(\mathbf{r} - \mathbf{r}'),\end{aligned} \tag{3}$$

where $G^{(2)}(0) \equiv G^{(2)}(\boldsymbol{r}, \boldsymbol{r})$, $G^{(3)}(\boldsymbol{r}, \boldsymbol{r}, \boldsymbol{r}) \equiv G^{(3)}(0)$, $\psi_0 \equiv \langle\psi\rangle|_{J=0} = 1$, and $\nabla \equiv \nabla_{\boldsymbol{r}}$. We have neglected $G^{(5)}$ as a cutoff of the hierarchy. Comparing with the 2nd-order equation (Wu & Zhang 2022), Equation (3) also contains $G^{(2)}G^{(4)}$ terms, and

$G^{(4)}$ in the delta source. As expected, Equation (3) reduces to that of the Gaussian approximation (Zhang et al. 2019), when all the higher order terms, such as $G^{(2)}G^{(2)}G^{(2)}$, $G^{(2)}G^{(3)}$, $G^{(4)}$, are dropped, Since Equation (3) contains $G^{(4)}$, it is not closed for $G^{(3)}$. To cutoff the hierarchy, we adopt Fry–Peebles ansatz (Fry & Peebles 1978)

$$\begin{aligned} & G^{(4)}(\boldsymbol{r}_1, \boldsymbol{r}_2, \boldsymbol{r}_3, \boldsymbol{r}_4) \\ & = R_a[G^{(2)}(\boldsymbol{r}_1, \boldsymbol{r}_2)G^{(2)}(\boldsymbol{r}_2, \boldsymbol{r}_3)G^{(2)}(\boldsymbol{r}_3, \boldsymbol{r}_4) \\ & + \text{sym. } (12 \quad \text{terms})] \\ & + R_b[G^{(2)}(\boldsymbol{r}_1, \boldsymbol{r}_2)G^{(2)}(\boldsymbol{r}_1, \boldsymbol{r}_3)G^{(2)}(\boldsymbol{r}_1, \boldsymbol{r}_4) \\ & + \text{sym. } (4 \quad \text{terms})], \end{aligned} \tag{4}$$

where R_a and R_b are dimensionless constants, and $(3R_a + R_b)/4 \simeq 2.5 \pm 0.5$ as constrained by observations (Fry 1983, 1984; Meiksin et al. 1992; Szapudi et al. 1992; Peebles 1993). The ansatz (4) leads to

$$\begin{aligned} & G^{(4)}(\boldsymbol{r}, \boldsymbol{r}, \boldsymbol{r}', \boldsymbol{r}'') = 2R_a G^{(2)}(0)G^{(2)}(\boldsymbol{r}, \boldsymbol{r}')G^{(2)}(\boldsymbol{r}', \boldsymbol{r}'') \\ & + 2R_a G^{(2)}(0)G^{(2)}(\boldsymbol{r}, \boldsymbol{r}'')G^{(2)}(\boldsymbol{r}', \boldsymbol{r}'') \\ & + 2(R_a + R_b)G^{(2)}(0)G^{(2)}(\boldsymbol{r}, \boldsymbol{r}')G^{(2)}(\boldsymbol{r}, \boldsymbol{r}'') \\ & + 2R_a G^{(2)}(\boldsymbol{r}, \boldsymbol{r}')G^{(2)}(\boldsymbol{r}, \boldsymbol{r}'')G^{(2)}(\boldsymbol{r}', \boldsymbol{r}'') \\ & + 2R_a G^{(2)}(\boldsymbol{r}, \boldsymbol{r}')^2 G^{(2)}(\boldsymbol{r}, \boldsymbol{r}'') + 2R_a G^{(2)}(\boldsymbol{r}, \boldsymbol{r}')G^{(2)}(\boldsymbol{r}, \boldsymbol{r}'')^2 \\ & + R_b G^{(2)}(\boldsymbol{r}, \boldsymbol{r}')^2 G^{(2)}(\boldsymbol{r}', \boldsymbol{r}'') + R_b G^{(2)}(\boldsymbol{r}, \boldsymbol{r}'')^2 G^{(2)}(\boldsymbol{r}', \boldsymbol{r}''), \end{aligned} \tag{5}$$

and

$$\begin{aligned} & G^{(4)}(\boldsymbol{r}, \boldsymbol{r}, \boldsymbol{r}, \boldsymbol{r}') = 3(2R_a + R_b)G^{(2)}(0)^2 G^{(2)}(\boldsymbol{r}, \boldsymbol{r}') \\ & + 6R_a G^{(2)}(0)G^{(2)}(\boldsymbol{r}, \boldsymbol{r}')^2 + R_b G^{(2)}(\boldsymbol{r}, \boldsymbol{r}')^3. \end{aligned} \tag{6}$$

Equation (3) also contains the squeezed $G^{(3)}(\boldsymbol{r}, \boldsymbol{r}, \boldsymbol{r}') = \lim_{\boldsymbol{r}'' \to \boldsymbol{r}} G^{(3)}(\boldsymbol{r}, \boldsymbol{r}', \boldsymbol{r}'')$ with three points being reduced to two. In observations and simulations $G^{(3)}(\boldsymbol{r}, \boldsymbol{r}, \boldsymbol{r}')$ cannot be resolved, (Gaztañaga et al. 2005; McBride et al. 2011a, 2011b; Yuan et al. 2017). To avoid the divergence, we adopt the Groth–Peebles ansatz (Groth & Peebles 1975, 1977)

$$\begin{aligned} & G^{(3)}(\boldsymbol{r}, \boldsymbol{r}', \boldsymbol{r}'') = Q[G^{(2)}(\boldsymbol{r}, \boldsymbol{r}')G^{(2)}(\boldsymbol{r}', \boldsymbol{r}'') \\ & + G^{(2)}(\boldsymbol{r}', \boldsymbol{r}'')G^{(2)}(\boldsymbol{r}'', \boldsymbol{r}) + G^{(2)}(\boldsymbol{r}'', \boldsymbol{r})G^{(2)}(\boldsymbol{r}, \boldsymbol{r}')], \end{aligned} \tag{7}$$

where the constant $Q \sim 1$ as constrained by observations. Then the squeezed 3PCF becomes

$$G^{(3)}(\boldsymbol{r}, \boldsymbol{r}, \boldsymbol{r}') = 2QG^{(2)}(0)G^{(2)}(\boldsymbol{r}, \boldsymbol{r}') + QG^{(2)}(\boldsymbol{r}, \boldsymbol{r}')^2, \tag{8}$$

consisting of regular $G^{(2)}(\boldsymbol{r}, \boldsymbol{r}')$. Substituting (5) (6) (8) into Equation (3), we obtain the closed equation of the 3PCF

$$\begin{aligned} & \nabla^2 G^{(3)}(\boldsymbol{r}, \boldsymbol{r}', \boldsymbol{r}'') + \boldsymbol{a}^{(3)} \cdot \nabla G^{(3)}(\boldsymbol{r}, \boldsymbol{r}', \boldsymbol{r}'') \\ & + 2g^{(3)}k_J^2 G^{(3)}(\boldsymbol{r}, \boldsymbol{r}', \boldsymbol{r}'') - \mathcal{A}^{(3)}(\boldsymbol{r}, \boldsymbol{r}', \boldsymbol{r}'') \\ & = -\frac{1}{\alpha}(2 - (1 + b)e + 3(2R_a + R_b)b^2 + 6R_a bG^{(2)}(\boldsymbol{r}, \boldsymbol{r}'') \\ & + R_b G^{(2)}(\boldsymbol{r}, \boldsymbol{r}'')^2)\delta^{(3)}(\boldsymbol{r} - \boldsymbol{r}')G^{(2)}(\boldsymbol{r}, \boldsymbol{r}'') \\ & - \frac{1}{\alpha}(2 - (1 + b)e + 3(2R_a + R_b)b^2 + 6R_a bG^{(2)}(\boldsymbol{r}, \boldsymbol{r}') \\ & + R_b G^{(2)}(\boldsymbol{r}, \boldsymbol{r}')^2)\delta^{(3)}(\boldsymbol{r} - \boldsymbol{r}'')G^{(2)}(\boldsymbol{r}, \boldsymbol{r}'), \end{aligned} \tag{9}$$

where

$$\begin{aligned} & \mathcal{A}^{(3)}(\mathbf{r}, \mathbf{r}', \mathbf{r}'') \\ & = [(2 + 2(3 + R_a + R_b - 4Q)b + 12(2R_a + R_b)b^2) \\ & \times (1 + b)^{-1} - 6e]\nabla G^{(2)}(\mathbf{r}, \mathbf{r}') \cdot \nabla G^{(2)}(\mathbf{r}, \mathbf{r}'') \\ & - [2k_J^2(1 + b)^{-1} - 6k_J^2(2R_a + R_b)b^2(1 + b)^{-1} + 2k_J^2 e \\ & - (1 + R_a + R_b - 2Q + 8(2R_a + R_b)b)c \\ & - 2(2R_a + R_b)(1 + b)|\mathbf{a}^{(2)}|^2 + 2f]G^{(2)}(\mathbf{r}, \mathbf{r}')G^{(2)}(\mathbf{r}, \mathbf{r}'') \\ & + R_a cG^{(2)}(\mathbf{r}', \mathbf{r}'')(G^{(2)}(\mathbf{r}, \mathbf{r}') + G^{(2)}(\mathbf{r}, \mathbf{r}'')) \\ & + [(R_a + R_b - 3Q - 1 + 10(2R_a + R_b)b)\mathbf{a}^{(2)} + 3\mathbf{a}^{(3)}] \\ & \cdot (\nabla G^{(2)}(\mathbf{r}, \mathbf{r}')G^{(2)}(\mathbf{r}, \mathbf{r}'') + \nabla G^{(2)}(\mathbf{r}, \mathbf{r}'')G^{(2)}(\mathbf{r}, \mathbf{r}')) \\ & + (2 - 3Q + R_a + R_b + 2(2R_a + R_b)b)\frac{b}{1 + b} \\ & \times (\nabla^2 G^{(2)}(\mathbf{r}, \mathbf{r}')G^{(2)}(\mathbf{r}, \mathbf{r}'') + \nabla^2 G^{(2)}(\mathbf{r}, \mathbf{r}'')G^{(2)}(\mathbf{r}, \mathbf{r}')) \\ & + R_a G^{(2)}(\mathbf{r}', \mathbf{r}'')\Bigg[\frac{b}{1 + b}(\nabla^2 G^{(2)}(\mathbf{r}, \mathbf{r}') + \nabla^2 G^{(2)}(\mathbf{r}, \mathbf{r}'')) \\ & + \mathbf{a}^{(2)} \cdot (\nabla G^{(2)}(\mathbf{r}, \mathbf{r}') + \nabla G^{(2)}(\mathbf{r}, \mathbf{r}''))\Bigg] \\ & + (2R_a + 8R_a b - Q)(1 + b)^{-1}[(|\nabla G^{(2)}(\mathbf{r}, \mathbf{r}')|^2 \\ & + G^{(2)}(\mathbf{r}, \mathbf{r}')\nabla^2 G^{(2)}(\mathbf{r}, \mathbf{r}'))G^{(2)}(\mathbf{r}, \mathbf{r}'') \\ & + (|\nabla G^{(2)}(\mathbf{r}, \mathbf{r}'')|^2 + G^{(2)}(\mathbf{r}, \mathbf{r}'')\nabla^2 G^{(2)}(\mathbf{r}, \mathbf{r}''))G^{(2)}(\mathbf{r}, \mathbf{r}')] \\ & + (R_a - Q)(1 + b)^{-1}[4(G^{(2)}(\mathbf{r}, \mathbf{r}') \\ & + G^{(2)}(\mathbf{r}, \mathbf{r}''))\nabla G^{(2)}(\mathbf{r}, \mathbf{r}') \cdot \nabla G^{(2)}(\mathbf{r}, \mathbf{r}'') \\ & + G^{(2)}(\mathbf{r}, \mathbf{r}')^2 \nabla^2 G^{(2)}(\mathbf{r}, \mathbf{r}'') + \nabla^2 G^{(2)}(\mathbf{r}, \mathbf{r}')G^{(2)}(\mathbf{r}, \mathbf{r}'')^2] \\ & + 24R_a b(1 + b)^{-1}(G^{(2)}(\mathbf{r}, \mathbf{r}') + G^{(2)}(\mathbf{r}, \mathbf{r}''))\nabla G^{(2)}(\mathbf{r}, \mathbf{r}') \\ & \cdot \nabla G^{(2)}(\mathbf{r}, \mathbf{r}'') + (4R_a c + 6k_J^2 R_a b(1 + b)^{-1})(G^{(2)}(\mathbf{r}, \mathbf{r}') \\ & + G^{(2)}(\mathbf{r}, \mathbf{r}''))G^{(2)}(\mathbf{r}, \mathbf{r}')G^{(2)}(\mathbf{r}, \mathbf{r}'') \\ & + R_a \mathbf{a}^{(2)} \cdot [8(\nabla G^{(2)}(\mathbf{r}, \mathbf{r}') \\ & + \nabla G^{(2)}(\mathbf{r}, \mathbf{r}''))G^{(2)}(\mathbf{r}, \mathbf{r}')G^{(2)}(\mathbf{r}, \mathbf{r}'') \\ & + 6(\nabla G^{(2)}(\mathbf{r}, \mathbf{r}'')G^{(2)}(\mathbf{r}, \mathbf{r}')^2 + \nabla G^{(2)}(\mathbf{r}, \mathbf{r}')G^{(2)}(\mathbf{r}, \mathbf{r}'')^2)] \end{aligned}$$

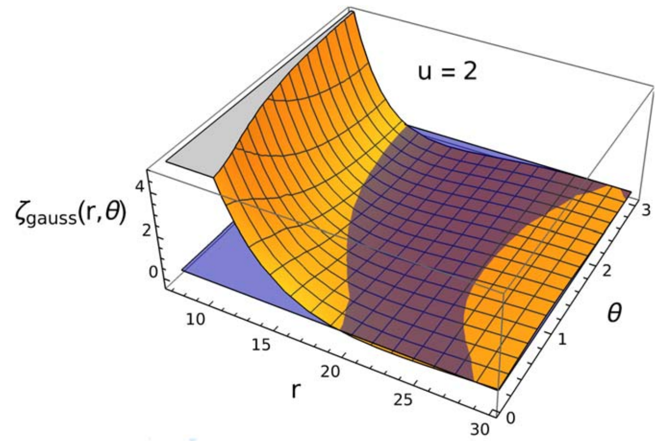

Figure 1. The Gaussian $\zeta(r,\ u,\ \theta)$ in the spherical coordinates with $u = 2$. Along the r-direction, $\zeta(r)$ becomes negative around $r = (14 \sim 27)h^{-1}$ Mpc forming a shallower U-shape. Along the θ-direction, $\zeta(\theta)$ decreases monotonously at small r, and oscillates at large r.

$$\begin{aligned}
&+\ R_a(1+b)^{-1}G^{(2)}(\mathbf{r}', \mathbf{r}'')(\nabla^2 G^{(2)}(\mathbf{r}, \mathbf{r}')G^{(2)}(\mathbf{r}, \mathbf{r}'')\\
&+ G^{(2)}(\mathbf{r}, \mathbf{r}')\nabla^2 G^{(2)}(\mathbf{r}, \mathbf{r}'')\\
&+\ 2\nabla G^{(2)}(\mathbf{r}, \mathbf{r}')\cdot\nabla G^{(2)}(\mathbf{r}, \mathbf{r}''))\\
&+ R_b(1+b)^{-1}G^{(2)}(\mathbf{r}', \mathbf{r}'')(|\nabla G^{(2)}(\mathbf{r}, \mathbf{r}')|^2\\
&+\ G^{(2)}(\mathbf{r}, \mathbf{r}')\nabla^2 G^{(2)}(\mathbf{r}, \mathbf{r}') + |\nabla G^{(2)}(\mathbf{r}, \mathbf{r}'')|^2 + G^{(2)}(\mathbf{r}, \mathbf{r}'')\nabla^2 G^{(2)}(\mathbf{r}, \mathbf{r}'\\
&+\ 2R_b(1+b)^{-1}[G^{(2)}(\mathbf{r}, \mathbf{r}')G^{(2)}(\mathbf{r}, \mathbf{r}'')(G^{(2)}(\mathbf{r}, \mathbf{r}')\nabla^2 G^{(2)}(\mathbf{r}, \mathbf{r}')\\
&+ G^{(2)}(\mathbf{r}, \mathbf{r}'')\nabla^2 G^{(2)}(\mathbf{r}, \mathbf{r}'')\\
&+\ 2|\nabla G^{(2)}(\mathbf{r}, \mathbf{r}')|^2 + 2|\nabla G^{(2)}(\mathbf{r}, \mathbf{r}'')|^2)\\
&+ 3(G^{(2)}(\mathbf{r}, \mathbf{r}')^2 + G^{(2)}(\mathbf{r}, \mathbf{r}'')^2)\nabla G^{(2)}(\mathbf{r}, \mathbf{r}')\cdot\nabla G^{(2)}(\mathbf{r}, \mathbf{r}'')]\\
&+\ R_b k_J^2(1+b)^{-1}(G^{(2)}(\mathbf{r}, \mathbf{r}')^2\\
&+ G^{(2)}(\mathbf{r}, \mathbf{r}'')^2)G^{(2)}(\mathbf{r}, \mathbf{r}')G^{(2)}(\mathbf{r}, \mathbf{r}'').
\end{aligned} \tag{10}$$

In Equations (9) and (2), $\boldsymbol{a}^{(3)} \equiv (1+b)^{-1}(\frac{2}{\psi_0^2}\nabla G^{(2)}(0) - \frac{2}{\psi_0^3}\nabla G^{(3)}(0))$, $\boldsymbol{a}^{(2)} \equiv (1+b)^{-1}\frac{2}{\psi_0^2}\nabla G^{(2)}(0)$, $b \equiv \frac{1}{\psi_0^2}G^{(2)}(0)$, $c \equiv \nabla^2 G^{(2)}(0)/[(1+b)\psi_0^2]$, $e \equiv G^{(3)}(0)/[(1+b)\psi_0^3]$, $f \equiv \nabla^2 G^{(3)}(0)/[(1+b)\psi_0^3]$, $g^{(3)} = \frac{1}{1+b} + \frac{c}{4k_J^2} - \frac{f}{3k_J^2} - \frac{e}{2}$, and α has absorbed a factor $(1+b)$. The six constants, $\boldsymbol{a}^{(3)}$, $\boldsymbol{a}^{(2)}$, b, c, e, f, are combinations of six unknowns: $G^{(2)}(0)$, $G^{(3)}(0)$, $\nabla G^{(2)}(0)$, $\nabla G^{(3)}(0)$, $\nabla^2 G^{(2)}(0)$ and $\nabla^2 G^{(3)}(0)$, which can be formally divergent, and are not directly measurable. These constants are inevitable in the perturbation approach to any field theory with interactions, and are often treated by some renormalization. In our case, we will set $g^{(3)} = 1$ as the renormalization of the Jeans wavenumber k_J, and take $(1+b)m$ as the renormalized mass. Equation (9) is a generalized Poisson equation (Hackbusch 2017) with the two delta sources located at $\boldsymbol{r}'$ and $\boldsymbol{r}''$ respectively, and the inhomogeneous term $\mathcal{A}^{(3)}$. Its structure is similar to the second order equation (Wu & Zhang 2022), but $\mathcal{A}^{(3)}$ has more terms. It also contains a convection term $\boldsymbol{a}^{(3)}\cdot\nabla G^{(3)}(\boldsymbol{r}, \boldsymbol{r}', \boldsymbol{r}'')$ and a gravitating term $g^{(3)}k_J^2 G^{(3)}(\boldsymbol{r}, \boldsymbol{r}', \boldsymbol{r}'')$. The Jeans wavenumber k_J determines the 3-point correlation length of the system of galaxies. $\alpha^{-1} \propto m$ determines the correlation amplitude at small scales, so that massive galaxies will have a higher amplitude of $G^{(3)}$. These two properties are analogous to those of 2PCF (Zhang 2007; Zhang & Li 2021).

When all nine nonlinear parameters (three from the ansatz) are neglected, Equation (9) reduces to the Gaussian approximation as the next order to the mean field theory (Zhang 2007; Zhang et al. 2019), $G^{(2)}(\boldsymbol{r}_1, \boldsymbol{r}_2) \propto \frac{\cos(\sqrt{2}k_J r_{12})}{r_{12}}$ with $r_{12} = |\boldsymbol{r}_1 - \boldsymbol{r}_2|$, and $G^{(3)}(\boldsymbol{r}, \boldsymbol{r}', \boldsymbol{r}'')$ given by the Groth–Peebles ansatz (7) with $Q = 1$. We plot the Gaussian $G^{(3)}$ in Figure 1.

Here the Gaussian approximation of the self-gravity density field is conceptually not the same as the Gaussian random process in statistics. A "reduced" 3PCF is often introduced as follows (Jing & Börner 2004; Wang et al. 2004; Gaztañaga et al. 2005; Nichol et al. 2006; McBride et al. 2011a, 2011b; Guo et al. 2014, 2016)

$$\begin{aligned}
&Q(\mathbf{r}, \mathbf{r}', \mathbf{r}'')\\
&\equiv \frac{G^{(3)}(\mathbf{r}, \mathbf{r}', \mathbf{r}'')}{G^{(2)}(\mathbf{r}, \mathbf{r}')G^{(2)}(\mathbf{r}', \mathbf{r}'') + G^{(2)}(\mathbf{r}', \mathbf{r}'')G^{(2)}(\mathbf{r}'', \mathbf{r}) + G^{(2)}(\mathbf{r}'', \mathbf{r})G^{(2)}(\mathbf{r}, \mathbf{r}')},
\end{aligned} \tag{11}$$

which is an extension of the Groth–Peebles ansatz (7). $Q(\boldsymbol{r}, \boldsymbol{r}', \boldsymbol{r}'') \neq 1$ is a criterion of non-Gaussianity.

3. Solution and Comparison with Observations

In a homogeneous and isotropic Universe, $G^{(2)}(\boldsymbol{r}, \boldsymbol{r}') = G^{(2)}(|\boldsymbol{r} - \boldsymbol{r}'|)$. The 3PCF is parameterized by $G^{(3)}(\boldsymbol{r}, \boldsymbol{r}', \boldsymbol{r}'') \equiv \zeta(r, u, \theta)$, where $r \equiv r_{12}$, $u = \frac{r_{13}}{r_{12}}$, $\theta = \cos^{-1}(\hat{\boldsymbol{r}}_{12}\cdot\hat{\boldsymbol{r}}_{13})$ (Marín 2011). For convenience, we take $\boldsymbol{r}'' = \boldsymbol{0}$ and put the vector $\boldsymbol{r}' - \boldsymbol{r}'' = \boldsymbol{r}'$ along the polar axis (see Figure 1 in Wu & Zhang (2022)), and write $G^{(2)}(\boldsymbol{r}, \boldsymbol{r}'') = \xi(r)$, $G^{(2)}(\boldsymbol{r}, \boldsymbol{r}') = \xi(l)$, $G^{(2)}(\boldsymbol{r}', \boldsymbol{r}'') = \xi(r') = \xi(ur)$, where $l \equiv |\boldsymbol{r} - \boldsymbol{r}'| = \beta r$, $\beta \equiv \sqrt{1 + u^2 - 2u\cos\theta}$. Then Equation (9) is written in spherical coordinates

$$\begin{aligned}
&\frac{1}{r^2}\frac{\partial}{\partial r}\left(r^2\frac{\partial}{\partial r}\zeta(r, u, \theta)\right) + \frac{1}{r^2\sin\theta}\frac{\partial}{\partial\theta}\left(\sin\theta\frac{\partial\zeta(r, u, \theta)}{\partial\theta}\right)\\
&+\ a_r^{(3)}\frac{\partial\zeta(r, u, \theta)}{\partial r} + 2k_J^2\zeta(r, u, \theta) - \mathcal{A}^{(3)}(r, u, \theta)\\
&= -\frac{b}{\alpha}(2 - (1+b)e + 4(3R_a + R_b)b^2)\\
&\quad\times\left(\frac{2}{|1-u|}\frac{\delta(\theta)}{\sin\theta} + 1\right)\frac{\delta(r)}{4\pi r^2},
\end{aligned} \tag{12}$$

where $a_r^{(3)}$ is the $r-$component of $\boldsymbol{a}^{(3)}$, and

$$
\begin{aligned}
&\mathcal{A}^{(3)}(r,\,u,\,\theta)\\
&=[(2+2(3+R_a+R_b-4Q)b+12(2R_a+R_b)b^2)\\
&\times(1+b)^{-1}-6e]\beta\xi'(l)\xi'(r)\\
&-[2k_J^2(1+b)^{-1}-(1+R_a+R_b-2Q+8(2R_a+R_b)b)c\\
&-2(2R_a+R_b)(1+b)(a_r^{(2)})^2\\
&-6k_J^2(2R_a+R_b)b^2(1+b)^{-1}+2f+2k_J^2e]\xi(l)\xi(r)\\
&+[(R_a+R_b-3Q-1+10(2R_a+R_b)b)a_r^{(2)}+3a_r^{(3)}]\\
&\times(\beta\xi'(l)\xi(r)+\xi(l)\xi'(r))\\
&+(2-3Q+R_a+R_b+2(2R_a+R_b)b)\frac{b}{1+b}\\
&\times\left[\left(\frac{2}{r}\xi'(r)+\xi''(r)\right)\xi(l)\right.\\
&+\left(\left(\frac{2}{r}\beta+\frac{2u}{\beta r}\cos\theta-\frac{u^2\sin^2\theta}{\beta^3 r}\right)\xi'(l)\right.\\
&\left.\left.+\left(\beta^2+\frac{u^2}{\beta^2}\sin^2\theta\right)\xi''(l)\right)\xi(r)\right]\\
&+(2R_a+8R_ab-Q)(1+b)^{-1}\\
&\times\left\{\left(\beta^2+\frac{u^2\sin^2\theta}{\beta^2}\right)\xi'(l)^2\xi(r)+\xi(l)\xi'(r)^2\right.\\
&+\left[\left(\frac{2}{r}\beta+\frac{2u}{\beta r}\cos\theta-\frac{u^2\sin^2\theta}{\beta^3 r}\right)\xi'(l)\right.\\
&\left.\left.+\left(\beta^2+\frac{u^2}{\beta^2}\sin^2\theta\right)\xi''(l)+\frac{2}{r}\xi'(r)+\xi''(r)\right]\xi(l)\xi(r)\right\}\\
&+(R_a-Q)(1+b)^{-1}\left[\left(\left(\frac{2}{r}\beta+\frac{2u}{\beta r}\cos\theta-\frac{u^2\sin^2\theta}{\beta^3 r}\right)\xi'(l)\right.\right.\\
&\left.+\left(\beta^2+\frac{u^2}{\beta^2}\sin^2\theta\right)\xi''(l)\right)\xi(r)^2\\
&\left.+\xi(l)^2\left(\frac{2}{r}\xi'(r)+\xi''(r)\right)+4(\xi(l)+\xi(r))\beta\xi'(l)\xi'(r)\right]\\
&+R_ab(1+b)^{-1}[24(\xi(l)+\xi(r))\beta\xi'(l)\xi'(r)\\
&+\xi(u\,r)\left(\left(\frac{2}{r}\beta+\frac{2u}{\beta r}\cos\theta-\frac{u^2\sin^2\theta}{\beta^3 r}\right)\xi'(l)\right.\\
&\left.\left.+\left(\beta^2+\frac{u^2}{\beta^2}\sin^2\theta\right)\xi''(l)+\frac{2}{r}\xi'(r)+\xi''(r)\right)\right]\\
&+(4R_ac+6k_J^2R_ab/(1+b))(\xi(l)+\xi(r))\xi(l)\xi(r)\\
&+R_aa_r^{(2)}[8(\beta\xi'(l)+\xi'(r))\xi(l)\xi(r)+6(\xi'(r)\xi(l)^2\\
&+\beta\xi'(l)\xi(r)^2)+\xi(u\,r)(\beta\xi'(l)+\xi'(r))]+\frac{R_b}{1+b}\left\{\xi(u\,r)\right.\\
&\times\left[\left(\beta^2+\frac{u^2\sin^2\theta}{\beta^2}\right)\xi'(l)^2+\xi'(r)^2\right.\\
&+\left(\frac{2}{r}\xi'(r)+\xi''(r)\right)\xi(r)\\
&+\left(\left(\frac{2}{r}\beta+\frac{2u}{\beta r}\cos\theta-\frac{u^2\sin^2\theta}{\beta^3 r}\right)\xi'(l)\right.\\
&\left.\left.+\left(\beta^2+\frac{u^2}{\beta^2}\sin^2\theta\right)\xi''(l)\right)\xi(l)\right]\\
&+6(\xi(l)^2+\xi(r)^2)\beta\xi'(l)\xi'(r)+2\xi(l)\xi(r)\\
&\times\left[2\left(\left(\beta^2+\frac{u^2\sin^2\theta}{\beta^2}\right)\xi'(l)^2+\xi'(r)^2\right)\right.\\
&+\left(\left(\frac{2}{r}\beta+\frac{2u}{\beta r}\cos\theta-\frac{u^2\sin^2\theta}{\beta^3 r}\right)\xi'(l)\right.\\
&\left.\left.\left.+\left(\beta^2+\frac{u^2}{\beta^2}\sin^2\theta\right)\xi''(l)\right)\xi(l)+\left(\frac{2}{r}\xi'(r)+\xi''(r)\right)\xi(r)\right]\right\}\\
&+\frac{R_bk_J^2}{1+b}(\xi(l)^2+\xi(r)^2)\xi(l)\xi(r)\\
&+R_ac\xi(u\,r)(\xi(l)+\xi(r))\\
&+\frac{R_a}{1+b}\xi(u\,r)\left[\left(\left(\frac{2}{r}\beta+\frac{2u}{\beta r}\cos\theta-\frac{u^2\sin^2\theta}{\beta^3 r}\right)\right.\right.\\
&\left.\times\xi'(l)+\left(\beta^2+\frac{u^2}{\beta^2}\sin^2\theta\right)\xi''(l)\right)\xi(r)\\
&\left.+\xi(l)\left(\frac{2}{r}\xi'(r)+\xi''(r)\right)+2\beta\xi'(l)\xi'(r)\right].
\end{aligned}
\tag{13}
$$

In observation and simulations, the ratio $u=2$ is often taken, so that $\zeta(r,\,u,\,\theta)$ will have only two variables. The 2PCF $\xi(r)$ is involved in Equation (12). Although $\xi(r)$ has been solved to various nonlinear orders (Zhang & Miao 2009; Zhang & Chen 2015; Zhang et al. 2019), we will use the observed $\xi(r)$ (Marín 2011) for a coherent comparison with observation.

An appropriate boundary condition is needed to solve Equation (12). Marín (2011) has observed the redshift-space $Q(s,\,u,\,\theta)$ of "DR7-Dim" (61,899 galaxies in the range $0.16\leqslant z\leqslant 0.36$) from SDSS in the domain $s\in[7.0,\,30.0]\,h^{-1}$Mpc, $\theta\in[0.1,\,3.04]$ at five respective values $s=7$, 10, 15, 20, 30 h^{-1} Mpc at a fixed $u=2$, where s is the redshift distance. (See Figure 6 and Figure 7 of Marín (2011).) s may differ from the real distance r due to the peculiar velocities. We will neglect this error and take $r=s$ in our computation. From this data, we get the fitted $Q(r,\,u,\,\theta)$, as well as $\zeta(r,\,u,\,\theta)$ via the relation (11), on the boundary of the domain, which is taken as

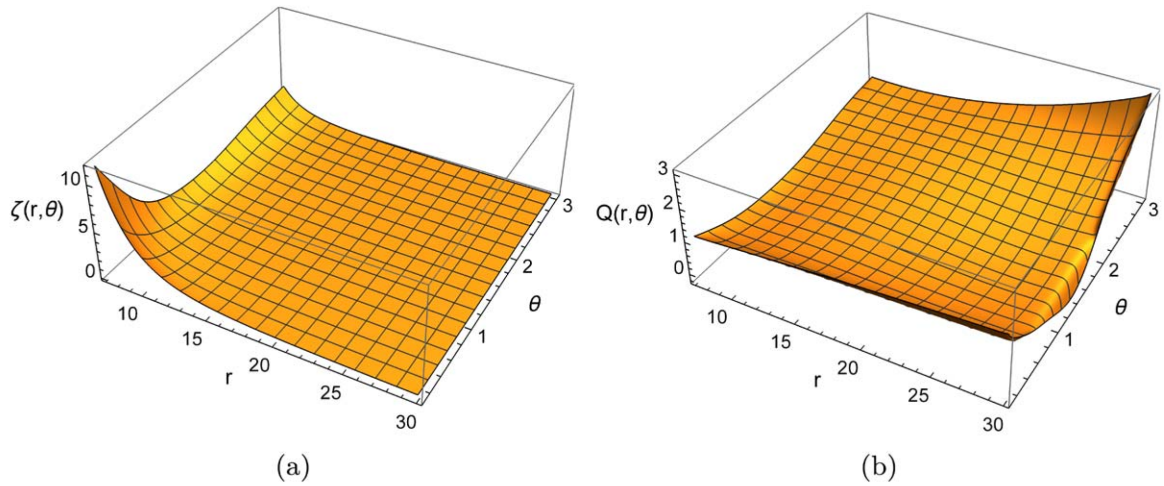

Figure 2. (a) The nonlinear $\zeta(r, u, \theta)$ (with fixed $u=2$) is positive, has a U-shape along θ, and decreases monotonously along r up to the range $r \leqslant 30\, h^{-1}$ Mpc of our computation. This behavior differs from Figure 1 of the Gaussian solution. (b) The reduced $Q(r, u, \theta) \neq 1$ exhibits a deeper U-shape along θ, varies non-monotonously along r, and its high values occur at large r where $\xi(r)$ is small.

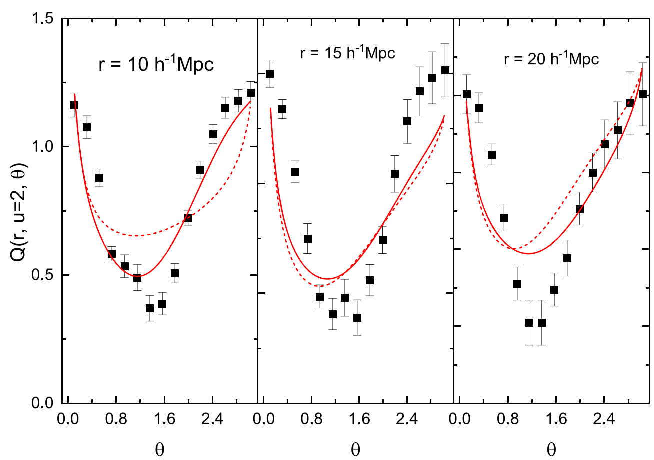

Figure 3. The solid line: $Q(r, u, \theta)$ from Equation (12). The dashed line: the second order solution from Figure 6 of Wu & Zhang (2022). Three plots are for $r = 10h^{-1}$Mpc, $15h^{-1}$Mpc, $20h^{-1}$Mpc, respectively. The dots: the SDSS data from Figure 6 and Figure 7 of Marín (2011), which are measured in the redshift space. Our solutions are of the real space. There are difference between the real and redshift spaces, which are neglected in this preliminary treatment here.

the boundary condition of Equation (12). The effect of the delta source is absorbed by the boundary condition (Hackbusch 2017; Zhang & Li 2021).

We solve Equation (12) numerically by the finite element method, and obtain the solution $\zeta(r, u, \theta)$ and the reduced $Q(r, u, \theta)$ defined by (11). To match the observational data (Marín 2011), using the method of χ^2 test, the parameters are chosen as follows: $a_r^{(3)} \simeq -4.4\, h$ Mpc^{-1}, $a_r^{(2)} \simeq 0.35\, h$ Mpc^{-1}, $b \simeq 0.73$, $c \simeq 0.03\, h^2$Mpc^{-2}, $e \simeq -6.9$, $Q \simeq 1.7$, $R_a \simeq 4.1$, $R_b \simeq -0.47$, $k_J \simeq 0.038\, h$Mpc^{-1}. In particular, the values of Q, R_a and R_b of the ansatz are consistent with that inferred from other surveys (Peebles 1993). Besides, the chosen k_J is also consistent the value used in our previously work on the 2PCF (Zhang 2007; Zhang & Miao 2009; Zhang & Chen 2015; Zhang et al. 2019). The parameter α has not been accurately fixed because the delta source has been absorbed into the boundary condition in our numeric solution (Hackbusch 2017; Zhang & Li 2021).

Figure 2 (a) shows the solution $\zeta(r, u, \theta)$ at fixed $u=2$ as a function of (r, θ). It is seen that $\zeta(r, u, \theta) > 0$ in the range of computation, and exhibits a shallow U-shape along the $\theta-$direction. This feature is consistent with observations (Guo et al. 2014, 2016). Along the $r-$direction $\zeta(r, u, \theta)$ decreases monotonously up to $30\, h^{-1}$ Mpc in the range. The highest values of $\zeta(r, u, \theta)$ occur at small r, just as $\xi(r)$ does. This is also expected since the correlations are stronger at small distance due to gravity.

Figure 2 (b) shows the nonlinear reduced $Q(r, u, \theta) \neq 1$, deviating from the Gaussianity $Q=1$. $Q(r, u, \theta)$ exhibits a deeper U-shape along θ, and varies non-monotonically along r. The variation along r is comparatively weaker than the variation along θ. These features are consistent with what have been observed (Marín 2011; McBride et al. 2011a, 2011b).

To compare with the observational data (Marín 2011), Figure 3 plots the solution $Q(r, u, \theta)$ as a function of θ at $r = 10, 15, 20\, h^{-1}$Mpc, respectively. It is seen that $Q(r, u, \theta)$ has a U-shape along $\theta = [0, 3]$, agreeing with the data. Overall, the equations of 3PCF gives a reasonable account of the data of galaxies with redshifts $0.16 \leqslant z \leqslant 0.36$. For a comparison, in Figure 3 we also plot the second order solution (dashed lines). Note that we have renormalized the parameters of the third order solution in this paper, the number of parameters also differs from that of the second order. It is clear that the third order solution fits the data ($\chi^2 = 470.9$) better than the second order one ($\chi^2 = 777.8$), especially at small scales, and the two solutions are close at large scales.

4. Conclusions and Discussions

Based on the density field Equation (1), we have derived Equation (3) of the 3-point correlation function $G^{(3)}$ of galaxies, up to the third order density fluctuation. This work is a continuation of the previous Gaussian approximation (Zhang et al. 2019), and the second order work (Wu & Zhang 2022).

By neglecting the 5PCF, adopting the Fry–Peebles ansatz to deal with the 4PCF, and the Groth–Peebles ansatz to deal with the squeezed 3PCF, respectively, we have made Equation (3) into the closed Equation (9). Aside the three parameters from the ansatz, there are six nonlinear parameters that occur inevitably in the perturbation treatment of a gravitating system. We carry out renormalization of the Jeans wavenumber and the mass. Although the terms $(\delta\psi)^3$ are included, nonlinear terms such as $(G^{(3)})^2$ do not appear in Equation (9) of $G^{(3)}$, and higher order terms than $(\delta\psi)^3$ are needed for $(G^{(3)})^2$ to appear.

We apply the equation to the system of galaxies, using the boundary condition inferred from SDSS DR7 (Marín 2011) for a consistent comparison. The solution $\zeta(r, u, \theta)$ exhibits a shallow U-shape along θ, and decreases monotonously along r. The reduced $Q(r, u, \theta)$ deviates from 1 of the Gaussian case, and exhibits a U-shape along θ. Along r, however, $Q(r, u, \theta)$ varies non-monotonically, scattering around 1.

It is interesting that the third order solution in this paper is quite close to the second order solution (Wu & Zhang 2022), especially at large scales. This indicates that the density field theory with increasing orders of perturbation provides a rather stable description of the nonlinear galaxy system. Besides, from the study on 3PCF and the previous work on 2PCF, it is seen that the static equations of correlation functions present a reasonable analytical account of the galaxy distribution at small redshifts. The future work will be application to new observational data, and extension to the case of expanding Universe.

Acknowledgments

Y.Z. is supported by NSFC (Grant Nos. 11675165, 11633001, and 11961131007), and in part by the National Key RD Program of China (2021YFC2203100).

References

Bernardeau, F., Colombi, S., Gaztañaga, E., & Scoccimarro, R. 2002, PhR, 367, 1
Bharadwaj, S. 1994, ApJ, 428, 419
Bharadwaj, S. 1996, ApJ, 472, 1
Binney, J. J., Dowrick, N., Fisher, A., & Newman, M. 1992, The Theory of Critical Phenomena (New York: Oxford Univ. Press)
Davis, M., & Peebles, P. J. E. 1977, ApJS, 34, 425
Fry, J. N. 1983, ApJ, 267, 483
Fry, J. N. 1984, ApJ, 279, 499
Fry, J. N. 1994, PhRvL, 73, 215
Fry, J. N., & Peebles, P. J. E. 1978, ApJ, 221, 19
Gaztañaga, E., Norberg, P., Baugh, C. M., & Croton, D. J. 2005, MNRAS, 364, 620
Goldenfeld, N. 1992, Lectures on Phase Transitions and the Renormalization Group (Frontiers in Physics), Vol. 85 (Oxford: Westview Press)
Groth, E. J., & Peebles, P. J. E. 1975, ApJ, 196, 1
Groth, E. J., & Peebles, P. J. E. 1977, ApJ, 217, 385
Guo, H., Li, C., Jing, Y. P., & Börner, G. 2014, ApJ, 780, 139
Guo, H., Zheng, Z., Behroozi, P. S, et al. 2016, ApJ, 813, 3
Hackbusch, W. 2017, Elliptic Differential Equations, Theory and Numerical Treatment (Berlin: Springer)
Inagaki, S. 1991, PASJ, 43, 661
Jing, Y. P., & Börner, G. 2004, ApJ, 607, 140
Marín, F. A. 2011, ApJ, 737, 97
McBride, C. K., Connolly, A. J., Gardner, J. P., et al. 2011a, ApJ, 726, 13
McBride, C. K., Connolly, A. J., Gardner, J. P., et al. 2011b, ApJ, 739, 85
Meiksin, A., Szapudi, I., & Szalay, A. S. 1992, ApJ, 394, 87
Nichol, R. C., Sheth, R. K., Suto, Y., et al. 2006, MNRAS, 368, 1507
Peebles, P. J. E. 1980, The Large-scale Structure of the Universe (Princeton, NJ: Princeton Univ. Press)
Peebles, P. J. E. 1993, Principles of Physical Cosmology (Princeton, NJ: Princeton Univ. Press)
Szapudi, I., Szalay, A. S., & Boschán, P. 1992, ApJ, 390, 350
Wang, Y., Yang, X., Mo, H. J., et al. 2004, MNRAS, 353, 287
Wu, S. G., & Zhang, Y. 2022, RAA, 22, 045015
Yuan, S., Eisenstein, D. J., & Garrison, L. H. 2017, MNRAS, 472, 577
Zhang, Y. 2007, A&A, 464, 811
Zhang, Y., & Chen, Q. 2015, A&A, 581, A53
Zhang, Y., Chen, Q., & Wu, S. G. 2019, RAA, 19, 53
Zhang, Y., & Li, B. C. 2021, PhRvD, 104, 123513
Zhang, Y., & Miao, H. X. 2009, RAA, 9, 501
Zinn-Justin, J. 1996, Quantum Field Theory and Critical Phenomena (New York: Oxford Univ. Press)